Int. J. Electrochem. Sci., 15 **(2020)** 9746 – 9758, doi: 10.20964/2020.10.58

International Journal of ELECTROCHEMICAL SCIENCE
www.electrochemsci.org

A Comprehensive Study on Surface Activity, Scale and Corrosion Inhibition Performance of N^1, $N^{1'}$-(ethane-1, 2-diyl)bis(ethane-1, 2-diaminium) *O*, *O*-di(phenyl/*p*-tolyl) phosphorodithioate

Wei Wei[1], *Chuan Lai*[1,2,*], *Lan Wang*[2], *Changlu Liu*[1], *Zhaoju Zhu*[1], *Yanchuan Gong*[1], *Xueyu Zhi*[1], *Feiyu Ren*[1], *Jiewen Jiang*[1]

[1] School of Chemistry and Chemical Engineering, Sichuan University of Arts and Science, Dazhou 635000, China
[2] DaZhou Quality Technical Supervision and Inspection Testing Center, Dazhou 635000, China
[*]E-mail: laichuanemail@163.com

Received: 24 June 2020 / *Accepted:* 9 August 2020 / *Published:* 31 August 2020

The scale and corrosion inhibitors, N^1, $N^{1'}$-(ethane-1, 2-diyl)bis(ethane-1, 2-diaminium) *O,O*-diphenylphosphorodithioate (I-inh) and N^1, $N^{1'}$-(ethane-1, 2-diyl)bis(ethane-1, 2-diaminium) *O,O*- di-*p*-tolylphosphorodithioate (II-inh) have been successfully synthesized by the reaction of phenol/ *p*-methylphenol with phosphorus pentasulfide and triethylenetetramine in toluene solution. Meanwhile, the scale inhibition and corrosion inhibition performance of I-inh and II-inh were evaluated in this work. The corrosion inhibition evaluated by potentiodynamic polarization and weight loss and measurements show that I-inh and II-inh both are mixed-type effective corrosion inhibitors for Q235 steel (235QS) corrosion in H_2SO_4 solution. The scale inhibition efficiency and corrosion inhibition efficiency increased with I-inh and II-inh concentration increasing. Additionally, these two scale and corrosion inhibitors can also be used as excellent surfactants, the surface tension of I-inh and II-inh at critical micelle concentration were 37.64 mN m^{-1} (17.14 mmol L^{-1}) and 35.40 mN m^{-1}(18.03 mmol L^{-1}), respectively. The scale inhibition performance of I-inh against $CaCO_3$ and $CaSO_4$ scale are better than that of II-inh under the same conditions.

Keywords: Synthesis; Surface activity; Scale inhibition; Corrosion inhibition.

1. INTRODUCTION

Materials corrosion is one of the most important problems faced by scientists in all over the world. Whenever materials are used, corrosion problems are inevitable, especially the corrosion problem of metal material is more prominent. Materials corrosion will not only cause economic losses,

but also bring safety hazards and environmental problems [1-3]. As an important metal material, Q235 steel is widely used in different fields resulting from its excellent mechanical property, availability and low cost. But the steel is easily serious corroded by different acid aggressive solutions. As is known to all, many methods and techniques have been reported for materials corrosion protection. Based on the corrosion of metal materials, using corrosion inhibitor for corrosion protection is one of the most convenient, effective and economic methods [4-6].

The research and application of corrosion inhibitors have attracted great attention. In recent years, different types of corrosion inhibitors have been developed and reported [7-15], such as 1,3-di(1-methyl-1-ethylamino-2-nundecyl-4,5-dihydro-imidazoline; 1-enthylamino-2-n-undecyl- 4,5-dihydro-iminazoline; 2-(3-Bromophenyl)-1-phenyl-1H-benzimidazole); 2-amino-4-chloro-benzothiazole; 2-(2-chlorophenyl)-1H-Benzimidazole; 1-phenyl-2-thiourea; 1,3-diisopropyl-2-thiourea; 2,2′-bipyridyl-5,5′-dimethylene-bis(N,N′-dimethylalkylammonium bromide); 2-hydroxy-N′-((thiophene-2-yl)methylene)benzohydrazide; acetohydroxamic acid, benzohydroxamic acid and oxalohydroxamic acid; Hydroxyethyl ammonium O,O′-diphenyl dithiophosphate. However, different corrosion inhibitors have their own advantages and disadvantages, such as pungent odor, low efficiency, high cost, chemical instability and other disadvantages.

Therefore, in order to develop new corrosion inhibitors with better performance, more economical and more applicable, N^1, $N^{1'}$-(ethane-1, 2-diyl)bis(ethane-1, 2-diaminium) *O*,*O*-diphenylphosphorodithioate (I-inh) and N^1, $N^{1'}$-(ethane-1, 2-diyl)bis(ethane-1, 2-diaminium) *O*,*O*- di-*p*-tolylphosphorodithioate (II-inh) would be synthesized in this paper. Meanwhile, the surface activity, scale and corrosion inhibition performance of I-inh and II-inh were evaluated in this work.

2. EXPERIMENTAL

2.1 Materials

In this work, all analytical grade chemicals used without further purification, including toluene, phenol, *p*-methylphenol, phosphorus pentasulphide, triethylenetetramine and concentrated sulfuric acid (98%). The test samples and working electrode using to potentiodynamic polarization and weight loss and measurements were prepared by Q235 steel (235QS) with the chemical compositions (wt.%) of Mn (0.531), Si (0.270), C (0.187), P (<0.040), S (<0.045) and Fe (Bal.).

2.2 Synthesis of I-inh and II-inh

According to synthesis methods reported in our previous works [1, 5 15, 16], the scale and corrosion inhibitor ($[(RO)_2PSS^-]_4\{[NH_3(CH_2)_2NH_2CH_2]^{2+}\}_2$, R= phenyl, p-methylphenyl), N^1, $N^{1'}$-(ethane-1, 2-diyl)bis(ethane-1, 2-diaminium) *O*,*O*- diphenylphosphorodithioate (I-inh) and N^1, $N^{1'}$-(ethane-1, 2-diyl)bis(ethane-1, 2-diaminium) *O*,*O*- di-*p*-tolylphosphorodithioate (II-inh) have been successfully synthesized by the reaction of *p*-methylphenol/phenol with phosphorus pentasulfide and

triethylenetetramine in toluene solution. Meanwhile, the synthetic route and chemical structures of $([(RO)_2PSS^-]_4\{[NH_3(CH_2)_2NH_2CH_2]^{2+}\}_2$ show in Figure 1.

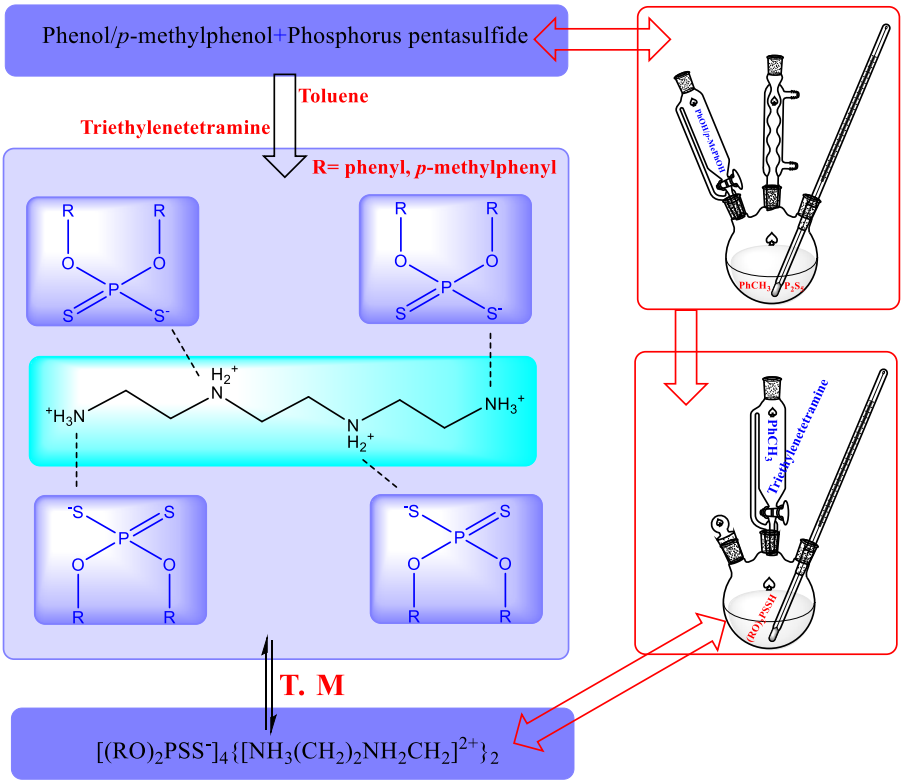

Figure 1. Schematic diagram for synthetic reaction of I-inh and II-inh.

2.3 Potentiodynamic polarization measurement

Potentiodynamic polarization measurement as one of the most commonly used methods for corrosion inhibition evaluation have been reported in various references [17-18]. This method is mainly used to evaluate the corrosion inhibition performance by obtaining corrosion current densities of working electrode corrosion in blank corrosion solution (i_0) and the corrosion solutions with different concentrations of inhibitor (i_i), the potential sweep rate was set as 0.5 mV s^{-1}. Meanwhile, the corrosion inhibition performance is presented by corrosion inhibition efficiency ($IE_{Corro\text{-}P}$, %), which can be calculated by equation (1) [17-18].

$$IE_{Corro-P}\ (\%) = \frac{i_0 - i_i}{i_0} \times 100 \qquad (1)$$

2.4 Weight loss measurement

Weight loss measurements as the most classical and accurate method to evaluate the corrosion inhibition have been described in many studies [19-20]. In this method, the corrosion rate (v_0, v_i) of metal specimens in the blank corrosion solution (v_0) and the corrosion solutions with different

concentrations of inhibitor (v_i) must be obtained before the corrosion inhibition efficiency ($IE_{\text{Corro-W}}$, %) can be calculated by equation (2) and (3) [19-20].

$$v_i = \frac{m_0 - m_i}{St} \quad (2)$$

$$IE_{\text{Corro-W}}\,(\%) = \frac{v_0 - v_i}{v_0} \times 100 \quad (3)$$

2.5 Surface active performance measurement

Surface activity performance is reflected by surface tension, which was measured by a surface Tensiometer (A101Plus, KINO Industry Co., Ltd, USA).) for different concentrations of I-inh and II-inh dissolved in double distilled water with a surface tension 70.39 mN m^{-1} at 30 °C.

2.6 Scale inhibition performance measurement

The scale inhibition performance of I-inh and II-inh against $CaCO_3$ scale and $CaSO_4$ scale were determined by static test method reported at different references [21-22]. According to this static test method, the remaining Ca^{2+} is titrated by EDTA standard solution and compared with the blank test. Furthermore, the scale inhibition efficiency (IE_{Scale}, %) can be calculated by the following equation.

$$IE_{\text{Scale}}\,(\%) = \frac{V_2 - V_1}{V_0 - V_1} \times 100 \quad (4)$$

In this equation, V_0, V_1 and V_2 are the volume of EDTA (V_0) without scale inhibitor at the beginning, (V_1) without scale inhibitor after incubation and (V_2) with scale inhibitor after incubation.

3. RESULTS AND DISCUSSION

3.1 Potentiodynamic polarization measurement

3.1.1 Effect of I-inh and II-inh concentration on $IE_{Corro-P}$

The potentiodynamic polarization curves for 235QS corrosion in 1.0 M H_2SO_4 with different concentrations (0 -180 mg L^{-1}) of I-inh and II-inh at 30 °C were shown in Figure 2 (a) and (b).

Based on potentiodynamic polarization measurement, the corrosion current density (i), corrosion potential (E vs SCE, V), cathodic and anodic Tafel slopes (β_c, β_a) can be obtained from potentiodynamic polarization curves. Meanwhile, the corrosion inhibition efficiency ($IE_{\text{Corro-P}}$, %) for 235QS corrosion in 1.0 M H_2SO_4 with different concentrations of I-inh and II-inh at 30 °C were calculated by equation (1) and listed in Table 1. From Table 1, Figure 2 (a) and (b), it can be seen that corrosion current density (i_0) of 235QS corrosion in 1.0 M H_2SO_4 is 2903.4 μA cm^{-2}. However, when the corrosion inhibitors of I-inh and II-inh had been added in the blank corrosion solution (1.0 M H_2SO_4), the corrosion current density (i_i) sharply decreased. With I-inh and II-inh concentration increases from 60 mg L^{-1} to 180 mg L^{-1}, the corrosion current density decreases from 397.4 μA cm^{-2} to 88.7 μA cm^{-2} and 427.4 μA cm^{-2} to 38.7μA cm^{-2}, respectively.

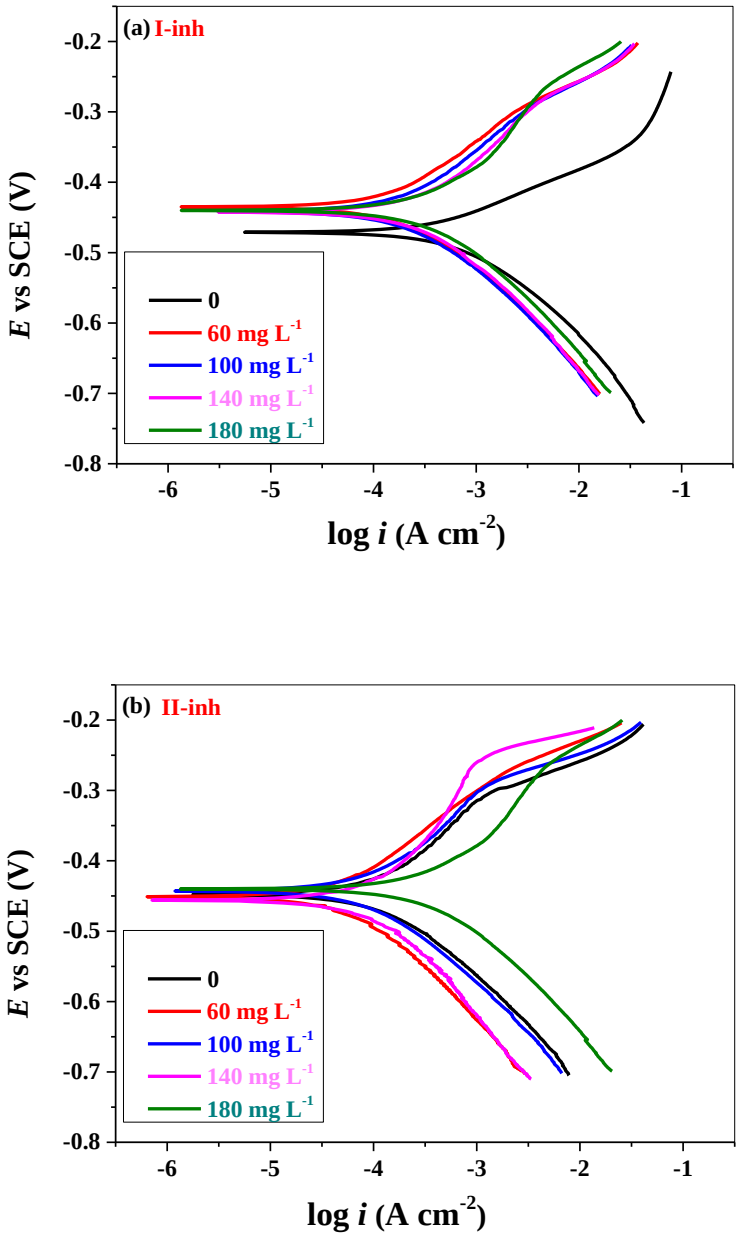

Figure 2. Potentiodynamic polarization curves for 235QS corrosion in 1.0 M H_2SO_4 with different concentrations of I-inh (a) and II-inh (b) at 30 °C.

The corrosion current directly determines the corrosion inhibition of I-inh and II-inh for 235QS corrosion in 1.0 M H_2SO_4. The decrease of corrosion current density is determined by the decrease of the corrosion rate of 235QS electrode corrosion in the corrosion medium (1.0 M H_2SO_4) with different concentrations of I-inh and II-inh. This shows that the corrosion inhibitors of I-inh and II-inh can effectively inhibit the corrosion of 235QS in 1.0 M H_2SO_4. Meanwhile, based on the corrosion current densities in Table 1 and calculated by equation (1), the corrosion inhibition efficiency ($IE_{Corro\text{-}P}$, %) for 235QS corrosion in 1.0 M H_2SO_4 with I-inh and II-inh (180 mg L^{-1}) at 30 °C are 96.9% and 98.7%, respectively. The increase of corrosion inhibition effect is due to the gradual adsorption of I-inh and II-

inh on 235QS surface, resulting into a dense self-protective film, which also indicates that I-inh and II-inh can act as effective inhibitor for 235QS in H_2SO_4 solution. Additionally, all corrosion potential exhibited in Table 1 shifts less than 36 mV ($\Delta E < 80$ mV), which reveals that I-inh and II-inh both are mixed-type corrosion inhibitor [5, 15].

Table 1. The polarization parameters for 235QS corrosion in 1.0 M H_2SO_4 with different concentrations of I-inh and II-inh at 30 °C.

/	c (mg L^{-1})	E (mV)	ΔE (mV)	i (μA cm^{-2})	Δi (μA cm^{-2})	β_a (mV dec^{-1})	β_c (mV dec^{-1})	$IE_{Corro-P}$ (%)
Blank	0	471	-	2903.4	-	139	149	-
I-inh	60	435	36	397.4	2506.08	110	117	86.3
	100	441	30	290.3	2613.13	119	118	90.0
	140	442	29	174.3	2729.16	135	117	94.0
	180	440	31	88.7	2814.73	141	125	96.9
II-inh	60	448	23	427.4	2476.08	115	119	86.0
	100	451	20	263.2	2640.29	129	119	90.9
	140	443	28	134.7	2768.77	133	129	95.4
	180	456	15	38.7	2864.73	148	140	98.7

3.1.2 Effects of temperature, H_2SO_4 concentration and immersion time on $IE_{Corro-P}$

The effect of temperature (T, °C), H_2SO_4 concentration (C_H, M) and immersion time (t, h) on corrosion inhibition efficiency ($IE_{Corro-P}$, %) for 235QS in 1.0 M H_2SO_4 with I-inh and II-inh (180 mg L^{-1}) by potentiodynamic polarization measurement were presented in Figure 3 (a), (b) and (c). From Figure 3 (a), (b) and (c), it not difficult to find that the corrosion inhibition efficiency ($IE_{Corro-P}$, %) decreases with the increase of temperature (T, °C) and H_2SO_4 concentration (C_H, M), and slightly fluctuated with the increase of immersion time (t, h).

Obviously, both I-inh and II-inh are exhibited excellent corrosion inhibition at lower temperatures, the corrosion inhibition efficiency for 235QS in H_2SO_4 solution with I-inh and II-inh (180 mg L^{-1}) at 15 °C are 98.9% and 99.8%. The corrosion inhibition efficiency of II-inh is higher than that of I-inh when the temperature is lower than 45 °C, and the opposite tendency appears at the temperature is higher than 45 °C showing in Figure 3 (a). With the temperature increase to 75 °C, the corrosion inhibition efficiency of I-inh and II-inh decrease to 63.4% and 54.0%, respectively.

With H_2SO_4 concentration (C_H, M) increases from 0.25 M to 3.0 M, the corrosion inhibition efficiency of II-inh is always higher than that of I-inh exhibiting in Figure 3 (b). When the H_2SO_4 concentration is higher than 2.0 M, the corrosion inhibition efficiency of I-inh and II-inh obviously decreases. The corrosion inhibition efficiency for 235QS in 0.25 M H_2SO_4 at with I-inh and II-inh (180 mg L^{-1}) at 30 °C are 98.6% and 99.5%, when the H_2SO_4 concentration increases to 3.0 M, the corrosion inhibition efficiency decreases to 75.9% and 81.42%.

The effect of immersion time (t, h) on corrosion inhibition efficiency ($IE_{Corro-P}$, %) for 235QS in 1.0 M H_2SO_4 with I-inh and II-inh (180 mg L^{-1}) at 30 °C was presented in Figure 3 (c). It can be found that the corrosion inhibition efficiency changed slightly with immersion time increasing. This

shows that the corrosion inhibitors of I-inh and II-inh both can be stable in H_2SO_4 solution and maintain the excellent corrosion inhibition for a long time. After 72 hours, the corrosion inhibition efficiency ($IE_{Corro\text{-}P}$, %) of I-inh and II-inh (180 mg L^{-1}) are as high as 95. 7% and 98.4%, respectively.

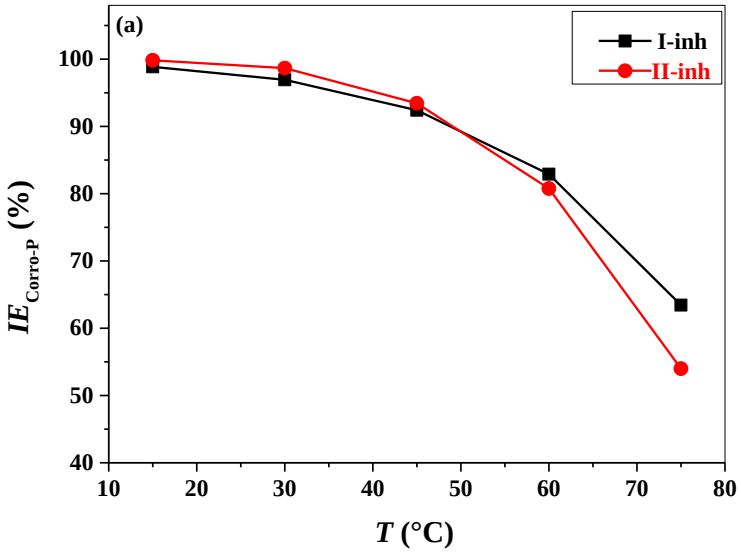

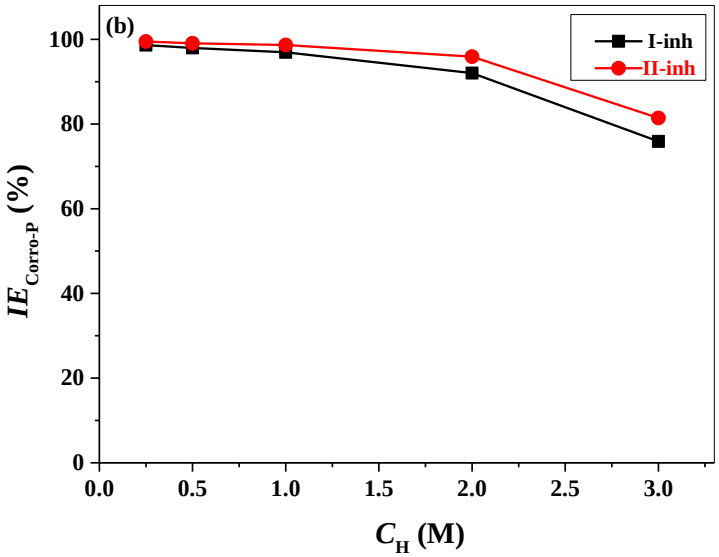

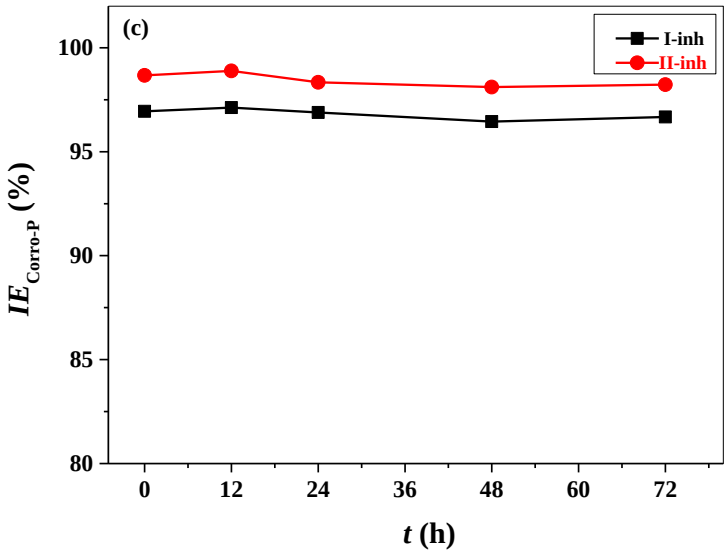

Figure 3. The effect of temperature (a), H_2SO_4 concentration (b) and immersion time (c) on corrosion inhibition efficiency ($IE_{Corro-P}$, %) for 235QS in H_2SO_4 solution with I-inh and II-inh (180 mg L^{-1}) by potentiodynamic polarization measurement.

3.2 Weight loss measurement

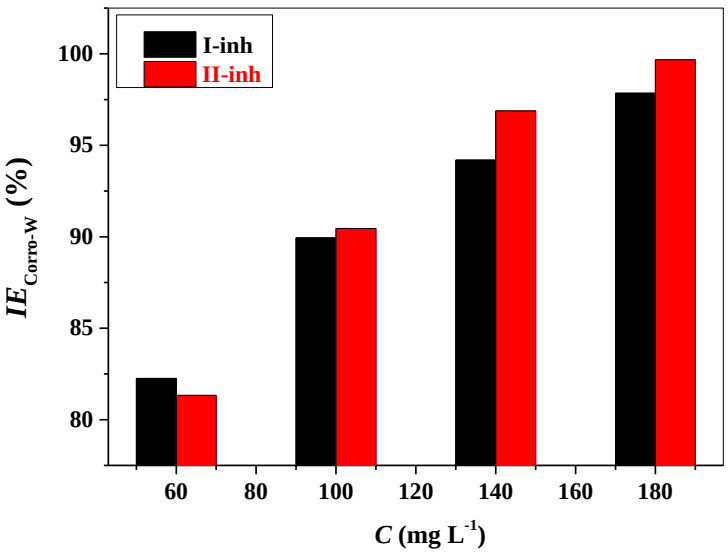

Figure 4. The effect of I-inh and II-inh concentration on corrosion inhibition efficiency ($IE_{Corro-W}$, %) for 235QS in 1.0 M H_2SO_4 with I-inh and II-inh by weight loss measurement.

The corrosion inhibition efficiency ($IE_{Corro-W}$, %) of 235QS corrosion in 1.0 M H_2SO_4 with various concentrations of I-inh and II-inh at 30 °C by weight loss measurement was exhibited in Figure 4. When the concentration of I-inh and II-inh both is 60 mg L^{-1}, the corrosion inhibition efficiency are

82.3% and 81.3%, respectively. Obviously, the corrosion inhibition efficiency of I-inh is higher than that of I-inh. When the concentration of inhibitors are higher than 100 mg L^{-1}, the corrosion inhibition efficiency of II-inh is higher than that of I-inh. With the concentration of corrosion inhibitors (I-inh and II-inh) increase to 180 mg L^{-1}, the corrosion inhibition efficiency reaches to 97.9% and 99.7%, respectively. The high corrosion inhibition efficiency indicates that both I-inh and II-inh can be used as the excellent corrosion inhibitors, while this result is consistent with the result of potentiodynamic polarization measurement. In addition, compared I-inh and II-inh with Sinapine Thiocyanate as corrosion inhibitor in 1.0 M H_2SO_4, that the corrosion inhibition performance of I-inh and II-inh in 1.0 M H_2SO_4 at100 mg L^{-1} (97.9% and 99.7%,) is better than that of Sinapine Thiocyanate in 1.0 M H_2SO_4 at 600 mg L^{-1} (95.7%)[23].

3.3 Adsorption isotherms

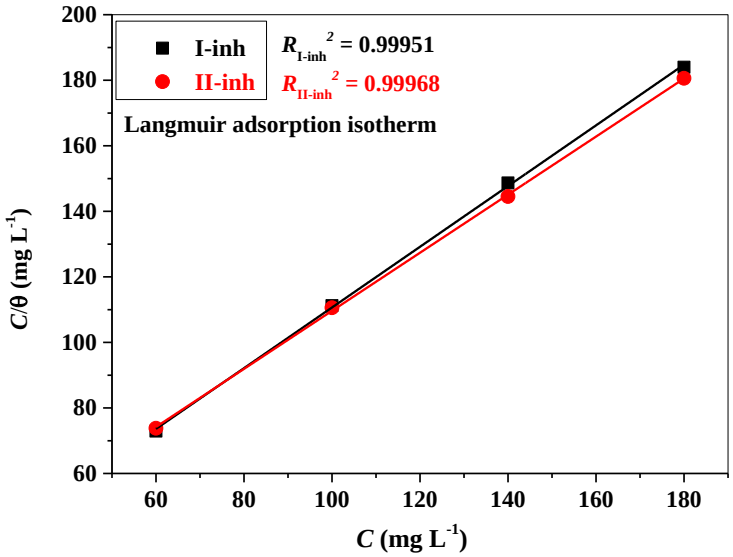

Figure 5. The plots of Langmui adsorption isotherms for I-inh and II-inh on 235QS surface in 1.0 M H_2SO_4 at 30 °C.

Table 2. Fitting results of Langmuir adsorption isotherm for I-inh and II-inh on 235QS in 1.0 M H_2SO_4 at 30 °C.

Inhibitors	*Isotherms*	*Pearson's* R^2	*Equation* ($y = a + b*x$)
I-inh	Langmuir	0.99951	y = 0.92624 * *x* + 18.0297
II-inh	Langmuir	0.99968	y = 0.88604 * *x* + 21.0338

In order to study the adsorption of corrosion inhibitor of I-inh and II-inh on 235QS surface, Here, the plots of Langmuir adsorption isotherm for I-inh and II-inh on 235QS surface in 1.0 M H_2SO_4 at 30 °C are presented in Figure 5, while the parameters obtained by fitting results are listed in Table 2. Based on Figure 5 Table 2, it not difficult to find that the adsorption models of I-inh and II-inh on

235QS surface most conforms to Langmuir adsorption isotherm. This is due to the fitting results show that R^2 is very close to 1 (R^2 =0.99951, 0.99968).

Furthermore, the adsorption free energy (ΔG) of I-inh and II-inh on 235QS surface in 1.0 M H_2SO_4 at 30 °C can be obtained according to the fitting results of Langmuir adsorption isotherm by equation (5) to (8) [15, 24-26]. Based on fitting results showing Table 3, ΔG can be calculated from equation (7), where the value of intercept ($1/K_0$) are 18.03 and 21.03 mg L^{-1}, and $1/K_0$ also can be used to calculate the K_1 by equation (8). The adsorption free energy (ΔG) of I-inh and II-inh on 235QS surface in 1.0 M H_2SO_4 at 30 °C are -37.64 kJ mol^{-1} and -37.45 kJ mol^{-1}, which also shows that the adsorption processes of I-inh and II-inh on235 QS surface both are physi- and chemisorption [15, 24-26].

$$\frac{c}{\theta} = \frac{1}{K_0} + c \quad (5)$$

$$\theta = \frac{v_0 - v_i}{v_0} \quad (6)$$

$$\Delta G = -RT\ln(55.5K_1) \quad (7)$$

$$K_1 = M_r \times K_0 \times 10^3 \ (\text{mol L}^{-1}) \quad (8)$$

Table 3. Fitting parameters and adsorption free energy of I-inh and II-inh on 235QS surface in 1.0 M H_2SO_4 at 30 °C by Langmuir adsorption isotherm.

Inhibitor	*M*r	$1/k_0$ (mg L^{-1}) $^{-1}$	k_1 (mol L^{-1}) $^{-1}$	ΔG (kJ mol^{-1})	Adsorption
I-inh	993	18.03	5.51×10^4	-37.64	Physi- and chemisorption
II-inh	1077	21.03	5.12×10^4	-37.45	Physi- and chemisorption

3.4 Surface active properties

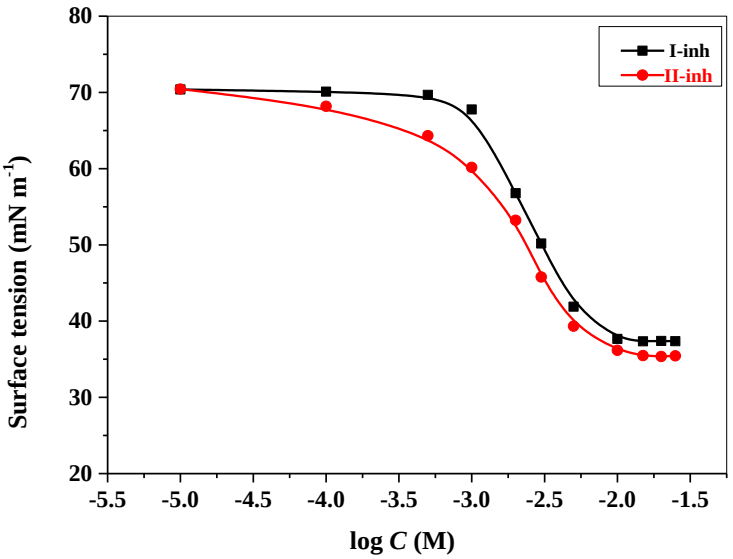

Figure 6. Variations in surface tension with I-inh and II-inh concentrations in double distilled water at 30 °C.

The surface tension (γ_{cmc}) of I-inh and II-inh was measured for a range of concentrations above and below the critical micelle concentration(cmc) and presented in Figure 6, which are 37.64 mN m^{-1} (I-inh, 17.14 mmol L^{-1}) and 35.40 mN m^{-1} (II-inh, 18.03 mmol L^{-1}). Meanwhile, the maximum surface pressure (π_{cmc}) of I-inh and II-inh can be calculated by the following equation: $\pi_{cmc} = \gamma_0 - \gamma_{cmc}$, where γ_0 is 70.39 mN m^{-1}, and the π_{cmc} are 32.75 mN m^{-1} (I-inh) and 34.99 mN m^{-1} (II-inh). The result indicates that the effective corrosion inhibitors of I-inh and II-inh also can be act as the excellent surfactant.

3.5 Surface active properties

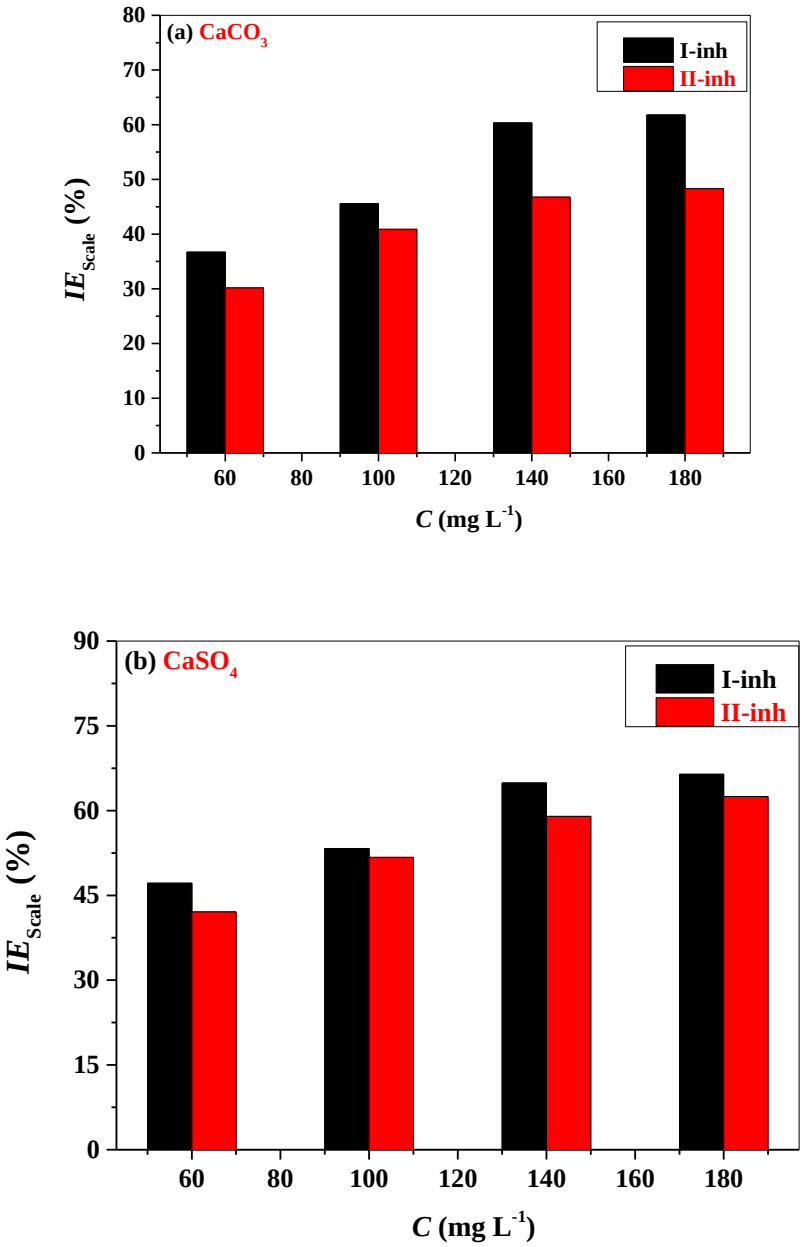

Figure 7. The effect of I-inh and II-inh concentration on the scale inhibition efficiency (*IE* scale, %) against $CaCO_3$ (a) and $CaSO_4$ (b).

The effect of I-inh and II-inh concentration on the scale inhibition efficiency (IE_{scale}, %) for against $CaCO_3$ and $CaSO_4$ scale were presented in Figure 7 (a) and (b). It can be seen from the Figure 7 (a) and (b) that the scale inhibition efficiency increases with the increase of scale inhibitors (I-inh and II-inh) concentration. When the scale inhibitors concentration reaches a certain value, the scale inhibition efficiency gradually tends to be stable. When the concentration of I-inh and II-inh increased from 60 mg L^{-1} to 180 mg L^{-1}, the scale inhibition efficiency for against $CaCO_3$ scale increased from 36.7% and 30.2 % to 61.78% and 48.3%, respectively, meanwhile, the scale inhibition efficiency for against $CaSO_4$ scale increased from 47.2% and 42.1% to 66.4% and 62.5%, respectively. By comparing Figure 7 (a) and (b), it can be seen that the performance of I-inh against $CaCO_3$ and $CaSO_4$ scale are better than that of II-inh under the same conditions.

4. CONCLUSIONS

N^1, $N^{1'}$-(ethane-1, 2-diyl)bis(ethane-1, 2-diaminium) *O*,*O*- diphenylphosphorodithioate (I-inh) and N^1, $N^{1'}$-(ethane-1, 2-diyl)bis(ethane-1, 2-diaminium) *O*,*O*- di-*p*-tolylphosphorodithioate (II-inh) as scale and corrosion inhibitors have been successfully synthesized. Meanwhile, the scale inhibition and corrosion inhibition performance of I-inh and II-inh were evaluated in this work. The corrosion inhibition evaluated by potentiodynamic polarization and weight loss and measurements show that I-inh and II-inh both are mixed-type effective corrosion inhibitors for Q235 steel in H_2SO_4 solution. The scale inhibition and corrosion inhibition efficiency increased with I-inh and II-inh concentration increasing. Additionally, these two scale and corrosion inhibitors can also be used as excellent surfactants, the surface tension of I-inh and II-inh at critical micelle concentration were 37.64 mN m^{-1} (17.14 mmol L^{-1}) and 35.40 mN m^{-1}(18.03 mmol L^{-1}), respectively. The scale inhibition performance of I-inh against $CaCO_3$ and $CaSO_4$ scale are better than that of II-inh under the same conditions.

ACKNOWLEDGEMENTS
This project is supported by Dazhou Scientific Research Project (Nos: 18ZDYF0009, 19YYJC0020, 19YYJC0013, 19ZDYF0014), Laboratories of Fine Chemicals and Surfactants in Sichuan Provincial Universities (2016JXZ03, 2018JXZ01), Sichuan University of Arts and Science (2018KC004Z, 2018KC005Z).

References

1. C. Wang, C. Lai, B. Xie, X. Guo, D. Fu, B. Li and S. Zhu, *Results. Phys*., 10 (2018) 558 - 567.
2. X. Su, C. Lai, L. Peng, H. Zhu, L. Zhou, L. Zhang, X. Liu and W. Zhang, *Int. J. Electrochem. Sci*., 11 (2016) 4828 - 4839.
3. I. B. Obot, I. B.Onyeachu, N. Wazzan and A. H. Al-Amri, *J. Mol. Liq*., 279 (2019) 190 - 207.
4. R. H. Khaled, A. M. Abdel-Gaber, H.T. Rahal and R. Awad, *Int. J. Electrochem. Sci*., 15 (2020) 6790 - 6801.
5. C. Lai, J. Cao, Y. Deng, Y. Yang, X. Wen, Z. Wang, C. Fan, Y. Shi, Y. Li, J. Li, C. Yang, Y. Yang, W. Pang and Y. Liu, *Int. J. Electrochem. Sci*., 14 (2019) 10259 - 10269.

6. C. Monticelli, A. Balbo, J. Esvan, C. Chiavari, C. Martini, F. Zanotto, L. Marvelli and L. Robbiola, *Corros. Sci*., 148 (2019) 144 - 158.
7. X. Wang, W. Zhuang, X. Luo, Y. Zhang, X. Sun and K.Li, *Int. J. Electrochem. Sci*., 15 (2020) 4338 - 4351
8. J. Zhang and H. Li, *Int. J. Electrochem. Sci*., 15 (2020) 4368 - 4378
9. S. Chen, S. Chen, H. Zhao, H. Wang, P. Wen and H. Li, *Int. J. Electrochem. Sci*., 15 (2020) 5208 - 5219.
10. J. Zhang and H. Li, *Int. J. Electrochem. Sci*., 15 (2020) 5362 - 5372.
11. D. Q. Huong, T. Duong and P. C. Nam, *ACS Omega*, 4 (2019) 14478 - 14489.
12. L. Feng, C. Yin, H. Zhang, Y. Li, X. Song, Q. Chen and H. Liu, *ACS Omega*, 3 (2018) 18990 - 18999.
13. A. K. Singh, S. Thakur, B. Pani, E. E. Ebenso, M. A. Quraishi and A. K. Pandey, *ACS Omega*, 3 (2018) 4695 - 4705.
14. D. K.Verma, A. A. Fantazi, C. Verma, F. Khan, A. Asatkar, C. M. Hussain and E. E. Ebenso, *J. Mol. Liq.,* 2020 (2020) 113651.
15. C. Lai, B. Xie and X. Guo, *Phosphorus. Sulfur*, 195 (2020) 107 - 114.
16. C. Lai, X. Guo, J. Wei, B. Xie, L. Zou, X. Li, Z. Chen and C. Wang, *Open Chem.*, 15 (2017) 263 - 271.
17. M. Abdallah, A. Fawzy and H. Hawsawi, *Int. J. Electrochem. Sci*., 15 (2020) 5650 - 5663.
18. X. Zeng, L. Zhu and X. Zheng, *Int. J. Electrochem. Sci*., 15 (2020) 5585 - 5596.
19. M. Mobin, M. Rizvi, L. O. Olasunkanmi and E. E. Ebenso, *ACS Omega*, 2 (2017) 3997 - 4008.
20. C. Shi, X. Song, Y. Kan, Y. Fan, X. Song, Y. Zhang and Z. Zhang, *Int. J. Electrochem. Sci*., 15 (2020) 4032 - 4055.
21. L. Wang, K. Cui, L. Wang, H. Li, S. Li, Q. Zhang and H. Liu, *Desalination*, 379 (2016) 75 - 84.
22. L. Wang, Q. Zhang, L. Wang, L. Wang, X. Wang, X. Ju, K. Cui and C. Zhu, Desalin. *Water. Treat*., 85 (2017) 36 - 45.
23. X.Jiang, C. Lai, Z. Xiang, J. Tang, L. Liu, Y. Gu, R. Wu, Z. Wu, J. Yuan, D. Hou and Y. Zhang, *Int. J. Electrochem. Sci.*, 13 (2018) 6462-6472.
24. X. Ma, J. Wang, J. Xu, J. Jing, J. Li, H. Zhu, S. Yu and Z. Hu, *ACS Omega*, 4 (2019) 21148 - 21160.
25. Q. Zhang, B. Hou, N. Xu, H. Liu and G. Zhang, *J. Taiwan Inst. Chem. Eng*., 96 (2019) 588 - 598.
26. Z. Sanaei, M. Ramezanzadeh, G. Bahlakeh and B. Ramezanzadeh, *J. Ind. Eng. Chem*., 69 (2019) 18 - 31.